J|A|C|S ARTICLES

Published on Web 10/26/2010

Effect of the Basic Residue on the Energetics, Dynamics, and Mechanisms of Gas-Phase Fragmentation of Protonated Peptides

Julia Laskin,*,† Zhibo Yang,† Tao Song,‡ Corey Lam,‡ and Ivan K. Chu‡

Fundamental Sciences Division, Pacific Northwest National Laboratory, Richland, Washington 99352, United States, and Department of Chemistry, The University of Hong Kong, Hong Kong, China

Received May 22, 2010; E-mail: julia.laskin@pnl.gov

Abstract: The effect of the basic residue on the energetics, dynamics, and mechanisms of backbone fragmentation of protonated peptides was investigated. Time-resolved and collision energy-resolved surface-induced dissociation (SID) of singly protonated peptides with the N-terminal arginine residue and their analogues, in which arginine is replaced with less basic lysine and histidine residues, was examined using a specially configured Fourier transform ion cyclotron resonance mass spectrometer (FTICR-MS). SID experiments demonstrated different kinetics of formation of several primary product ions of peptides with and without arginine residue. The energetics and dynamics of these pathways were determined from Rice−Ramsperger−Kassel−Marcus (RRKM) modeling of the experimental data. Comparison between the kinetics and energetics of fragmentation of arginine-containing peptides and the corresponding methyl ester derivatives provides important information on the effect of dissociation pathways involving salt bridge (SB) intermediates on the observed fragmentation behavior. Because pathways involving SB intermediates are characterized by low threshold energies, they efficiently compete with classical oxazolone and imine/enol pathways of arginine-containing peptides on a long time scale of the FTICR instrument. In contrast, fragmentation of histidine- and lysine-containing peptides is largely determined by canonical pathways. Because SB pathways are characterized by negative activation entropies, fragmentation of arginine-containing peptides is kinetically hindered and observed at higher collision energies as compared to their lysine- and histidine-containing analogues.

Introduction

Structural characterization of peptides is a focus of both fundamental and applied research in mass spectrometry. Gas-phase fragmentation of protonated peptide molecules has been extensively studied phenomenologically,[1−5] and the energetics and dynamics of fragmentation have been determined for a number of model systems.[6−8] Low-energy dissociation of protonated peptide ions is dominated by charge-directed processes. Mechanisms of peptide fragmentation are commonly discussed within the framework of the "mobile proton" model[2,9−11] and neighboring group interactions.[1] According to the mobile proton model, the ionizing proton is initially localized on the most basic site of the peptide. Dissociation is initiated by the transfer of the ionizing proton to the amide nitrogen or the carbonyl oxygen atom of the corresponding peptide bond. In the absence of strongly basic residues, the proton in the protonated peptide is not localized, but migrates along the peptide bond, inducing cleavages at the various amide bonds.[12−14] However, when the protonated peptide contains a strongly basic residue such as arginine (R) or lysine (K), the proton is sequestered at the basic site. As a result, the initial proton-transfer step in peptides containing basic residues is associated

† Pacific Northwest National Laboratory.
‡ The University of Hong Kong.

(1) O'Hair, R. A. J. *J. Mass Spectrom.* **2000**, *35*, 1377–1381.
(2) Wysocki, V. H.; Tsaprailis, G.; Smith, L. L.; Breci, L. A. *J. Mass Spectrom.* **2000**, *35*, 1399–1406.
(3) Schlosser, A.; Lehmann, W. D. *J. Mass Spectrom.* **2000**, *35*, 1382–1390.
(4) Polce, M. J.; Ren, D.; Wesdemiotis, C. *J. Mass Spectrom.* **2000**, *35*, 1391–1398.
(5) Paizs, B.; Suhai, S. *Mass Spectrom. Rev.* **2005**, *24*, 508–548.
(6) (a) Price, W. D.; Williams, E. R. *J. Phys. Chem. A* **1997**, *101*, 8844–8852. (b) Schnier, P. D.; Price, W. D.; Jockusch, R. A.; Williams, E. R. *J. Am. Chem. Soc.* **1996**, *118*, 7178–7189.
(7) (a) Laskin, J. *Eur. J. Mass Spectrom.* **2004**, *10*, 259–267. (b) Laskin, J.; Denisov, E.; Futrell, J. *J. Am. Chem. Soc.* **2000**, *122*, 9703–9714. (c) Laskin, J.; Bailey, T. H.; Denisov, E. V.; Futrell, J. H. *J. Phys. Chem. A* **2002**, *106*, 9832–9836. (d) Laskin, J.; Denisov, E.; Futrell, J. H. *Int. J. Mass Spectrom.* **2002**, *219*, 189–201. (e) Laskin, J. *J. Phys. Chem. A* **2006**, *110*, 8554–8562.
(8) Laskin, J. Energy and Entropy Effects in the Gas Phase Dissociation of Peptides and Proteins. In *Principles of Mass Spectrometry Applied to Biomolecules*; Laskin, J., Lifshitz, C., Eds.; John Wiley and Sons: New York, 2006.
(9) Burlet, O.; Orkiszewski, R. S.; Ballard, K. D.; Gaskell, S. J. *Rapid Commun. Mass Spectrom.* **1992**, *6*, 658–662.
(10) Dongre, A. R.; Jones, J. L.; Somogyi, A.; Wysocki, V. H. *J. Am. Chem. Soc.* **1996**, *118*, 8365–8374.
(11) Harrison, A. G.; Yalcin, T. *Int. J. Mass Spectrom. Ion Processes* **1997**, *16* (5−166), 339–347.
(12) Alexander, A. J.; Thibault, P.; Boyd, R. K. *Rapid Commun. Mass Spectrom.* **1989**, *3*, 30–34.
(13) Ballard, K. D.; Gaskell, S. J. *Int. J. Mass Spectrom. Ion Processes* **1991**, *111*, 173–189.
(14) Dongré, A. R.; Jones, J. L.; Somogyi, Á.; Wysocki, V. H. *J. Am. Chem. Soc.* **1996**, *118*, 8365–8374.

10.1021/ja104438z

with a higher barrier, resulting in the increased stability of the peptide toward fragmentation.[10,15]

Fragmentation of arginine- and lysine-containing peptides has attracted significant attention because most bottom-up protein sequencing applications in mass spectrometry use trypsin that cleaves protein backbone at arginine or lysine.[16] Tandem mass spectrometry (MS/MS) is subsequently used for identification of tryptic peptides.[17] It has been demonstrated that poor collision-induced dissociation (CID) spectra with limited structural information are often obtained when the number of ionizing protons is less than or equal to the number of basic residues in the peptide.[18] Knowledge of fragmentation energetics, dynamics, and mechanisms is the basis for interpreting and accurately predicting the MS/MS spectra of complex molecules.[19,20] Differences in the dissociation behavior of peptides with and without R are often attributed to the inability of the proton to migrate along the peptide backbone and direct dissociation when the basic arginine residue is present in the sequence.[21] Vachet and Glish proposed that charge-directed pathways are responsible for the decomposition of peptides that do not contain R, while charge-remote mechanisms are dominant for arginine-containing peptides.[22]

Several charge-remote dissociation pathways of protonated arginine-containing peptides have been extensively discussed. These include selective cleavages at the aspartic and glutamic acid residues,[15,23−25] loss of methanesulfenic acid from the oxidized methionine residue,[26] and some pathways responsible for the loss of phosphoric acid from phosphorylated peptides.[27] Charge-remote preferential bond cleavages often prevent the formation of sequence ions, thereby hindering peptide identification.

Another group of peptide fragmentation pathways involves salt bridge (SB) intermediates formed by deprotonation of the C-terminal carboxyl group. For example, elimination of the C-terminal amino acid residue resulting in formation of $b_n + H_2O$ ions from arginine-containing peptides involves SB intermediates.[28−30] The formation of these product ions is detrimental to peptide identification because they may be confused with y-ions. Farrugia and O'Hair demonstrated that other backbone fragments may be formed through SB intermediates.[31] Specifically, they found that singly protonated RG and GR yield identical low-energy CID spectra and proposed a mechanism that rationalizes this behavior. According to this mechanism, a SB intermediate is formed by proton transfer from the C-terminal carboxyl group. The SB formation is attributed to the presence of the arginine residue that sequesters the ionizing proton, which facilitates proton transfer from the C-terminal carboxyl group. The SB intermediate undergoes cyclization followed by rearrangement and formation of a mixed-anhydride intermediate from which the fragmentation takes place. A similar mechanism was proposed by Feng et al. to rationalize fragmentation of lithiated dipeptides.[32] In contrast with selective fragmentation pathways resulting in formation of characteristic products, SB pathways are charge-directed and yield the same products as classical oxazolone mechanisms[33,34] and, hence, are difficult to distinguish experimentally.

Recently, Bythell et al. reported the first computational study describing pathways involving SB and anhydride intermediates in dissociation of small G_nR ($n = 1-4$) peptides.[35] They examined the energetics of three amide bond cleavage mechanisms involving SB, anhydride, and imine enol intermediates and showed that all three mechanisms are less energetically demanding than the classical oxazolone pathway. [We note parenthetically that because both the classical oxazolone and the imine/enol pathway result in formation of fragment ions that have the same structure,[35] it is difficult if at all possible to distinguish between these mechanisms experimentally. In this study, we will refer to these pathways collectively as to canonical dissociation pathways to distinguish them from reaction channels involving SB intermediates.] However, they also found that SB pathways are characterized by more negative activation entropies. It is not clear whether the competition between different dissociation mechanisms is controlled by the energetics or by entropy effects that are particularly important for complex ions.[36]

Here, we address this question by comparing the energetics and dynamics of canonical and SB pathways of peptides differing only by the type of the basic residue in the sequence. Our results indicate that SB pathways efficiently compete with canonical pathways when arginine is present in the sequence. Dissociation parameters were obtained from time-resolved and collision energy-resolved surface-induced dissociation (SID) experiments combined with Rice−Ramsperger−Kassel−Marcus (RRKM) modeling of the experimental data. Previously, we showed that fast ion activation by collision with a surface combined with the long and variable time scale of a Fourier transform ion cyclotron resonance mass spectrometer (FTICR-MS) is perfectly suited for studying the energetics and dynamics of peptide fragmentation.[6,8] Because substitution of arginine with less basic lysine and histidine residues has a significant effect

(15) Tsaprailis, G.; Nair, H.; Somogyi, A.; Wysocki, V. H.; Zhong, W. Q.; Futrell, J. H.; Summerfield, S. G.; Gaskell, S. J. *J. Am. Chem. Soc.* **1999**, *121*, 5142–5154.
(16) Aebersold, R.; Goodlett, D. R. *Chem. Rev.* **2001**, *101*, 269–296.
(17) Wysocki, V. H.; Cheng, G.; Zhang, Q.; Herrmann, K. A.; Beardsley, R. L.; Hilderbrand, A. E. Peptide Fragmentation Overview. In *Principles of Mass Spectrometry Applied to Biomolecules*; Laskin, J., Lifshitz, C., Eds.; John Wiley & Sons., Inc.: Hoboken, NJ, 2006.
(18) Kapp, E. A.; Schutz, F.; Reid, G. E.; Eddes, J. S.; Moritz, R. L.; O'Hair, R. A. J.; Speed, T. P.; Simpson, R. J. *Anal. Chem.* **2003**, *75*, 6251–6264.
(19) Huang, Y. Y.; Triscari, J. M.; Tseng, G. C.; Pasa-Tolic, L.; Lipton, M. S.; Smith, R. D.; Wysocki, V. H. *Anal. Chem.* **2005**, *77*, 5800–5813.
(20) Laskin, J.; Futrell, J. H. *Mass Spectrom. Rev.* **2003**, *22*, 158–181.
(21) Tang, X. J.; Thibault, P.; Boyd, R. K. *Anal. Chem.* **1993**, *65*, 2824–2834.
(22) Vachet, R. W.; Asam, M. R.; Glish, G. L. *J. Am. Chem. Soc.* **1996**, *118*, 6252–6256.
(23) Yu, W.; Vath, J. E.; Huberty, M. C.; Martin, S. A. *Anal. Chem.* **1993**, *65*, 3015–3023.
(24) Qin, J.; Chait, B. T. *J. Am. Chem. Soc.* **1995**, *117*, 5411–5412.
(25) Summerfield, S. G.; Whiting, A.; Gaskell, S. J. *Int. J. Mass Spectrom. Ion Processes* **1997**, *162*, 149–161.
(26) Lioe, H.; Laskin, J.; Reid, G. E.; O'Hair, R. A. J. *J. Phys. Chem. A* **2007**, *111*, 10580–10588.
(27) Palumbo, A. M.; Tepe, J. J.; Reid, G. E. *J. Proteome Res.* **2008**, *7*, 771–779.
(28) Thorne, G. C.; Ballard, K. D.; Gaskell, S. J. *J. Am. Soc. Mass. Spectrom.* **1990**, *1*, 249–257.
(29) Ballard, K. D.; Gaskell, S. J. *J. Am. Chem. Soc.* **1992**, *114*, 64–71.
(30) Gonzalez, J.; Besada, V.; Garay, H.; Reyes, O.; Padron, G.; Tambara, Y.; Takao, T.; Shimonishi, Y. *J. Mass Spectrom.* **1996**, *31*, 150–158.
(31) Farrugia, J. M.; O'Hair, R. A. J. *Int. J. Mass Spectrom.* **2003**, *222*, 229–242.
(32) Feng, W. Y.; Gronert, S.; Fletcher, K. A.; Warres, A.; Lebrilla, C. B. *Int. J. Mass Spectrom.* **2003**, *222*, 117–134.
(33) Yalcin, T.; Khouw, C.; Csizmadia, I. G.; Peterson, M. R.; Harrison, A. G. *J. Am. Soc. Mass Spectrom.* **1995**, *6*, 1165–1174.
(34) Nold, M. J.; Wesdemiotis, C.; Yalcin, T.; Harrison, A. G. *Int. J. Mass Spectrom. Ion Processes* **1997**, *164*, 137–153.
(35) Bythell, B. J.; Suhai, S.; Somogyi, A.; Paizs, B. *J. Am. Chem. Soc.* **2009**, *131*, 14057–14065.
(36) Laskin, J.; Futrell, J. H. *J. Phys. Chem. A* **2003**, *107*, 5836–5839.

on the primary fragmentation pathways, it is difficult to select systems for comparison. Peptide ions examined in this study were carefully selected from a number of candidates containing basic residues at the N- or C-terminus. The criteria used in the selection process are discussed in the Results section.

In this study, we report the first experimental determination of the energy and entropy effects associated with different mechanisms of peptide backbone fragmentation. We demonstrate that pathways involving SB intermediates are characterized by low threshold energies but are kinetically hindered. In contrast, canonical pathways are associated with high-energy barriers and large, positive activation entropies. Because dissociation of arginine-containing peptides proceeds via kinetically hindered low-energy channels, high internal excitation often is required to obtain the average rate constant sampled experimentally. As a result, the apparent increase in the amount of collision energy required to observe fragmentation of arginine-containing precursor ions in a mass spectrometer often is determined by the activation entropy rather than by the energy threshold for dissociation.

Experimental Section

Surface-Induced Dissociation Experiments. SID experiments were conducted on a specially fabricated 6T FTICR mass spectrometer described in detail elsewhere.[37] The SID target is introduced through a vacuum interlock assembly and positioned at the rear trapping plate of the ICR cell. Ions are electrosprayed at atmospheric pressure and transferred into the vacuum system via an electrodynamic ion funnel.[38] Two quadrupoles following the ion funnel provide collisional focusing and mass selection of the ion of interest. Collisional octopole held at elevated pressure (about $(2-5) \times 10^{-3}$ Torr) is used for accumulation of mass-selected ions and collisional relaxation of any internal energy possessed by ions generated by electrospray ionization prior to their injection into the ICR cell. Mass-selected ions were accumulated for 0.2−1 s, extracted from the accumulation octopole, transferred into the ICR cell, and allowed to collide with the surface. Scattered ions were captured by raising the potentials on the front and rear trapping plates of the ICR cell by 10−20 V. Time-resolved mass spectra were acquired by varying the delay between the gated trapping and the excitation/detection event (the reaction delay) from 1 ms to 1 s. Immediately following the fragmentation delay, ions were excited through a broadband chirp and detected. The collision energy is defined by the difference between the potential applied to the accumulation quadrupole and the potential applied to the rear trapping plate and the SID target.

The self-assembled monolayer surface of 1-dodecanethiol (HSAM) was prepared on a single gold {111} crystal (Monocrystals, Richmond Heights, OH) using a standard procedure. The target was cleaned in a UV cleaner (model 135500, Boekel Industries Inc., Feasterville, PA) for 10 min and allowed to stand in a solution of 1-dodecanethiol for 10 h. The target was removed from the SAM solution and washed ultrasonically in ethanol for 10 min to eliminate extra layers.

Chemicals. Angiotensin III (RVYIHPF) and leucine enkephalin derivatives, RYGGFL and KYGGFL, were purchased from Sigma/Aldrich (St. Louis, MO). RFGGFL, RFGGFL-OMe, RYGGFL-OMe, KYGGFL-OMe, HVYIHPF, and HVYIHPF-OMe were synthesized according to literature procedures.[39] Fmoc-protected amino acids and the Wang resin were purchased from Advanced ChemTech (Louisville, KY). Samples were dissolved either in pure methanol or in a 70:30 (v/v) or 50:50 (v/v) methanol:water solution containing 1% acetic acid to a final concentration of ca. 50 μM. A syringe pump (Cole Parmer, Vernon Hills, IL) was used for direct infusion of the electrospray samples at flow rates ranging from 20 to 50 μL/h.

Theoretical Calculations. Molecular mechanics modeling was performed on an SGI Onyx 3200 workstation running Insight II/Discover (97.0, Accelrys Software Inc., San Diego, CA). Initial structures of the neutral and protonated peptides were built using the Biopolymer builder of Insight II (Biosym Technologies, San Diego, CA). Both initial and final structures were energy minimized using the CFF91 force field[40] for RYGGFL and KYGGFL and the Amber force field[41] for RVYIHPF and HVYIHPF peptides; the quasi-Newton−Raphson (VA09A) minimization algorithm was used in this study.[42] Conformational space of protonated peptides was explored using simulated annealing. Molecular dynamics (MD) simulations were performed at 1000 K in a vacuum with a 1.0 fs time step. Conformations were saved at 2 ps intervals over a 20 ns dynamics run, cooled to 300 K in 5 ps, and then energy minimized. Forty lowest-energy structures out of 10 000 minimized structures of RVYIHPF and HVYIHPF and 10 low-energy conformers out of 1000 minimized structures of RYGGFL and KYGGFL were selected for density functional theory (DFT) optimization at the B3LYP/3-21G level of theory. DFT calculations were carried out using NWChem (version 5.1.1) developed and distributed by the Pacific Northwest National Laboratory (PNNL).[43] Final geometries and single-point energies of 10 low-energy structures of RVYIHPF and HVYIHPF and four low-energy structures of RYGGFL and KYGGFL were obtained by subsequent optimization of these structures at the B3LYP/6-31G(d) level of theory; single-point energy calculations were carried out at the B3LYP/6-31++G(d, p) level of theory.

RRKM Modeling. Time-dependent survival curves (SCs) and fragmentation efficiency curves (TFECs) were constructed from experimental mass spectra by plotting the relative abundance of the corresponding ion as a function of collision energy for each delay time. TFECs were modeled using an RRKM-based approach described elsewhere.[44,45] First, the microcanonical rate coefficient, $k(E)$, was calculated as a function of internal energy using the microcanonical RRKM/QET expression.[46] Next, the survival probability of the precursor ion as a function of the internal energy of the precursor ion and the experimental observation time (t_r), $F(E, t_r)$, was calculated from the rate-energy $k(E)$ dependency, taking into account radiative decay of the excited ion population. The internal energy deposition function was described by the following analytical expression:

$$P(E,E_{coll}) = \frac{1}{C}(E - \Delta)^l \exp\left(-\frac{(E - \Delta)}{f(E_{coll})}\right) \quad (1)$$

where l and Δ are parameters, $C = \Gamma(l + 1)[f(E_{coll})]^{l+1}$ is a normalization factor, and $f(E_{coll})$ has the form:

(37) Laskin, J.; Denisov, E. V.; Shukla, A. K.; Barlow, S. E.; Futrell, J. H. *Anal. Chem.* **2002**, *74*, 3255–3261.
(38) Shaffer, S. A.; Tang, K. Q.; Anderson, G. A.; Prior, D. C.; Udseth, H. R.; Smith, R. D. *Rapid Commun. Mass Spectrom.* **1997**, *11*, 1813–1817.
(39) Chan, W. C.; White, P. D. *Fmoc Solid Phase Peptide Synthesis: A Practical Approach*; Oxford: New York, 2000.
(40) Schmidt, A. B.; Fine, R. M. *Mol. Simul.* **1994**, *13*, 347–365.
(41) Cornell, W. D.; Cieplak, P.; Bayly, C. I.; Gould, I. R.; Merz, K. M., Jr.; Ferguson, D. M.; Spellmeyer, D. C.; Fox, T.; Caldwell, J. W.; Kollman, P. A. *J. Am. Chem. Soc.* **1995**, *117*, 5179–5197.
(42) Fletcher, R. FORTRAN Subroutines for Minimization by Quasi-Newton Methods, U.K. Atom Energy Authority Research Group, NAERE R7125, 1972; p 29.
(43) Bylaska, E. J.; et al. *NWChem, A Computational Chemistry Package for Parallel Computers, Version 5.1*; Pacific Northwest National Laboratory: Richland, WA, 2007.
(44) Laskin, J.; Byrd, M.; Futrell, J. H. *Int. J. Mass Spectrom.* **2000**, *196*, 285–302.
(45) Laskin, J.; Futrell, J. H. *J. Phys. Chem. A* **2000**, *104*, 5484–5494.
(46) Baer, T.; Hase, W. L. *Unimolecular Reaction Dynamics: Theory and Experiments*.; Oxford University Press: New York, 1996; p 438.

$$f(E_{coll}) = A_2E_{coll}^2 + A_1E_{coll} + A_0 \quad (2)$$

where A_0, A_1, and A_2 are parameters, and E_{coll} is the collision energy.

We have shown previously that this analytical form for the collisional energy deposition function has enough flexibility to reproduce experimental fragmentation efficiency curves obtained using both gas-phase collisional activation and SID.[7,44] The overall signal intensity at a given collision energy, $I(E_{coll})$, was obtained using eq 3:

$$I_i(E_{coll}) = \int_0^\infty F(E,t)P(E,E_{coll})\,dE \quad (3)$$

Vibrational frequencies of the peptide were adopted from our previous study.[47] Vibrational frequencies for the transition state were estimated by removing one C−N stretch (reaction coordinate) from the parent ion frequencies, as well as scaling all frequencies in the range of 500−1000 cm^{-1} to obtain the best fit with experimental data.

TFECs were constructed using this procedure and compared to the experimental data. The internal energy deposition function was determined by fitting the experimental SCs of the singly protonated RVYIHPF and leucine enkephalin, for which the dissociation parameters are known from our previous studies,[7e,47] and kept the same for all reaction times. The fitting parameters included critical energies and activation entropies for different dissociation channels of the precursor ion. They were varied until the best fit to experimental TFECs was obtained.

Results

Survival Curves. In this study, we examined the effect of the basic residue on the cleavage of the same amide bond along the peptide backbone by comparing fragmentation of RYGGFL and KYGGFL (R versus K), RVYIHPF, and HVYIHPF (R versus H). Relative stabilities of protonated RYGGFL, KYGGFL, RVYIHPF, and HVYIHPF toward fragmentation are compared in Figure 1. Substitution of R with the less basic K and H residues results in ca. 11 eV shift of the SCs. This observation is consistent with previous studies showing similar trends in SCs for protonated peptides.[10,15,47−49] Higher stability of R-containing peptides toward fragmentation is the basis of the mobile proton model, which states that because of the difference in proton affinities of R and K, more energy is required to mobilize the proton in RYGGFL and RVYIHPF as compared to KYGGFL and HVYIHPF. However, our previous work demonstrated that activation entropy plays a significant role in determining the relative stability of protonated peptides toward fragmentation.[36] Dissociation parameters obtained from RRKM modeling of the experimental SCs are summarized in Table 1. Consistent with our previous study,[49a] substitution of arginine with a less basic residue has a pronounced effect on the activation entropy and only a minor effect on the dissociation energy. It should be noted that modeling of time-resolved SCs provides information on the total decomposition rate of precursor ions. Because (per the following discussion) substitution of R with K or H has a dramatic effect on the dissociation pathways of these peptides, the observed differences in the overall stability of peptides toward fragmentation could be simply related to differences in the fragmentation behavior. To address this question in more detail, we compared experimental TFECs obtained for selected fragment ions.

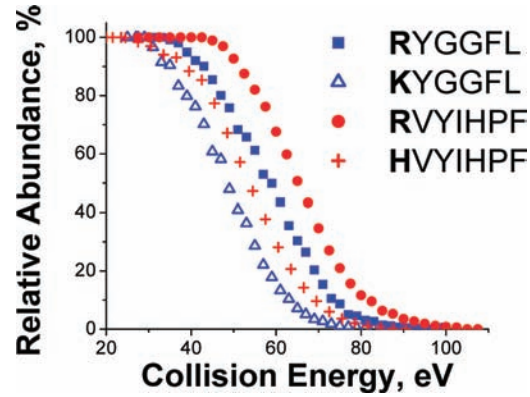

Figure 1. SCs for protonated precursor ions of RVYIHPF (red ●), HVYIHPF (red +), RYGGFL (blue ■), and KYGGFL (blue △) on the HSAM surface at a reaction delay of 1 s.

Table 1. Dissociation Parameters for the Total Decomposition of Different Protonated Peptides Examined in This Study[a]

	RYGGFL	KYGGFL	RVYIHPF	HVYIHPF
E_0, eV	1.68	1.71	1.62	1.56
$\Delta S^{\ddagger}$, eu[b]	9.3	17	−6.6	2.9
A, s^{-1}	3×10^{15}	1×10^{17}	1×10^{12}	1×10^{15}

[a] The estimated uncertainties are ±7% for threshold energies and ±3 eu for activation entropies. [b] eu = entropy units = cal/(mol K); activation entropies and pre-exponential factors at 450 K.

Specifically for each pair of precursors, we selected product ions for comparison if they corresponded to cleavage of the same amide bond and were produced directly from the precursor ion (primary fragments). It has been demonstrated that SB structures play an important role in gas-phase dissociation of arginine-containing singly protonated peptides.[31] O'Hair and co-workers showed that SB structures are formed by proton transfer from the C-terminal carboxyl group. They proposed that cyclization and rearrangement of the SB structure results in formation of a mixed-anhydride intermediate from which fragmentation takes place. Methylation of the C-terminus blocks the SB formation and switches off dissociation pathways that proceed through the SB intermediate. However, proton transfer from acidic side chains (e.g., serine, tyrosine, aspartic, and glutamic acid) can, in principle, promote the formation of SB intermediates. To distinguish between mechanisms involving SB structures and other dissociation pathways, we examined fragmentation of both peptides with the C-terminal carboxyl groups and their methyl ester derivatives. Finally, to eliminate the possibility of the SB formation involving the tyrosine side chain, we replaced the tyrosine residue with phenylalanine and examined the kinetics of fragmentation of KFGGFL, RFGGFL, and RFGGFL-OMe (data not shown). However, we found that both the overall stability toward dissociation and the fragment distribution were independent of this substitution, suggesting the side chain of tyrosine does not promote the formation of SB structures. Although the following discussion will focus on the protonated KYGGFL and RYGGFL and RYGGFL-OMe, we note that similar results were obtained for KFGGFL, RFGGFL, and RFGGFL-OMe analogues.

KYGGFL and RYGGFL. Figure 2 shows SID spectra of YGGFL analogues corresponding to 50% fragmentation. Dissociation of KYGGFL (Figure 2a) is dominated by the formation of the y_5 ion, internal b-, a-ions of YGGF sequence (y_5, b_4) and

(47) Laskin, J.; Bailey, T. H.; Futrell, J. H. *Int. J. Mass Spectrom.* **2004**, *234*, 89–99.
(48) Gu, C. G.; Somogyi, A.; Wysocki, V. H.; Medzihradszky, K. F. *Anal. Chim. Acta* **1999**, *397*, 247–256.
(49) (a) Bailey, T. H.; Laskin, J.; Futrell, J. H. *Int. J. Mass Spectrom.* **2003**, *222*, 313–327. (b) Laskin, J.; Bailey, T. H.; Futrell, J. H. *Int. J. Mass Spectrom.* **2006**, *249*, 462–472.

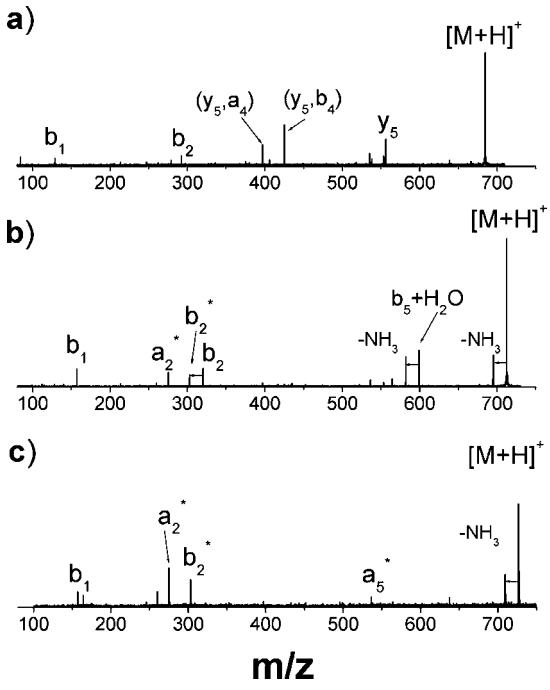

Figure 2. SID spectra corresponding to 50% fragmentation obtained on the HSAM surface at 1 s delay time for (a) KYGGFL, 49 eV; (b) RYGGFL, 57 eV; and (c) RYGGFL-OMe, 64 eV ($b_n^* = b_n - NH_3$; $a_n^* = a_n - NH_3$); (y_5, a_4) and (y_5, a_4) correspond to the internal b- and a-ion of YGGF sequence, respectively.

(y_5, a_4), and the b_2 ion. Higher-energy products include b_n (n = 1, 3−5), a_n (n = 1, 2, 5), $a_n - NH_3$ (n = 2, 5), $b_n - H_2O$ (n = 2−5), $b_5 + H_2O$, and a number of internal fragments and immonium ions. A similar fragmentation pattern (not shown) was observed for the methyl ester derivative of KYGGFL with $b_5 + H_2O$ being the only product ion that disappears upon methylation. In contrast, strikingly different fragment distribution is observed when the N-terminal lysine is replaced with the arginine. Low-energy dissociation channels of RYGGFL (Figure 2b) include loss of NH_3 and water from the protonated precursor and formation of $b_5 + H_2O$, $b_5 + H_2O - NH_3$, b_5, b_2, and b_1 fragment ions. Other abundant product ions produced at higher collision energies include $b_n - NH_3$ (n = 1−5), $a_n - NH_3$ (n = 1, 2, 4, 5), $b_4 + H_2O$, and $b_4 + H_2O - NH_3$. In contrast with KYGGFL, methylation of the C-terminal carboxyl group has a profound effect on the product distribution of RYGGFL (Figure 2c). Low-energy channels of RYGGFL-OMe include loss of NH_3 and the formation of $a_5 - NH_3$, $b_2 - NH_3$, $a_2 - NH_3$, and b_1 ions. In addition, an unassigned fragment ion at m/z 260.141 is observed in the spectrum. Product ions of RYGGFL-OMe produced by secondary fragmentation include $b_1 - NH_3$, $a_1 - NH_3$, $b_4 - NH_3$, F, y_1 ions, along with YGG and $YGGF_a$ internal fragments.

The disappearance of the $b_5 + H_2O$ and its subsequent fragments upon C-terminal methylation of RYGGFL and KYGGFL is not surprising because the formation of $b_n + H_2O$ ions involves a SB structure produced by proton transfer from the C-terminal carboxyl group that is blocked by methylation.[28−30] However, suppression of the formation of b_2 and b_5 ions from RYGGFL-OMe is rather unexpected and indicates these backbone fragments are formed through SB intermediates involving the C-terminal carboxyl group.[31] This finding is consistent with the recent computational study of fragmentation mechanisms of arginine-containing peptides that showed in the presence of a basic arginine residue pathways involving SB and anhydride intermediates become energetically favorable.[35]

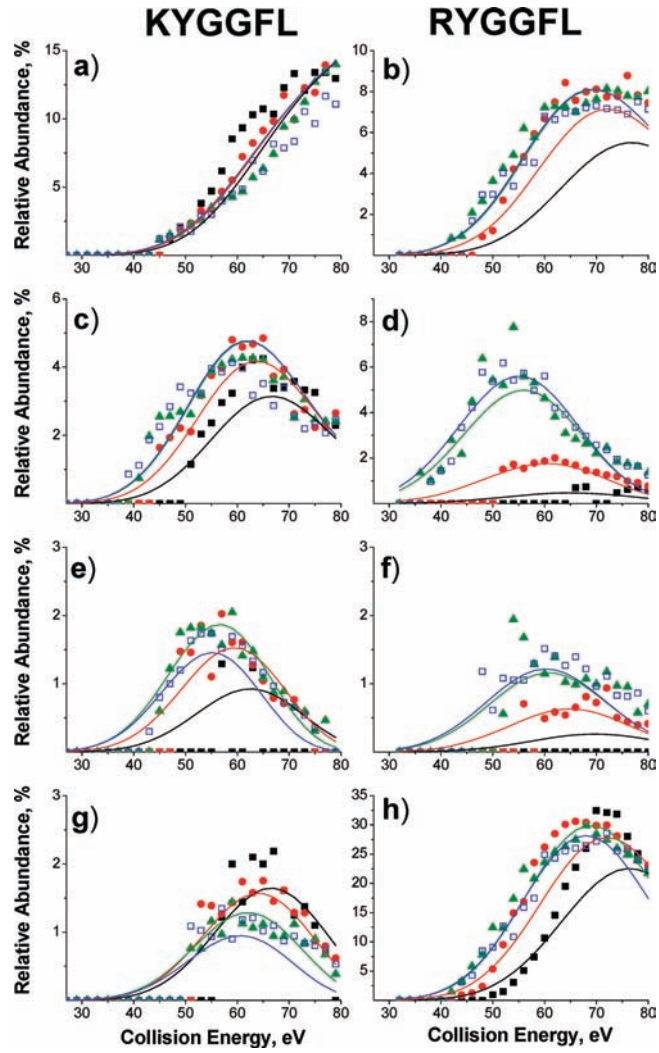

Figure 3. TFECs obtained for (a,b) b_1; (c,d) b_2; (e,f) b_5; (g,h) $b_5 + H_2O$ fragment ions of KYGGFL and RYGGFL. The results are shown for delay times of 1 ms (■), 10 ms (red ●), 100 ms (green ▲), and 1 s (blue □). Solid lines show RRKM modeling results for the corresponding delay times (refer to section KYGGFL and RYGGFL).

Because dissociation pathways of KYGGFL and RYGGFL are strikingly different, it is difficult to compare the overall stability of these peptides toward fragmentation. In contrast, comparison of the energetics and dynamics of formation of fragment ions common for both precursors is straightforward and reveals the effect of the basic residue on the energetics and mechanisms of specific dissociation channels. Because b_1, b_2, b_5, and $b_5 + H_2O$ are the only common primary products observed in SID spectra of both peptides, we examined the kinetics of formation of these fragment ions using time-resolved and collision energy-resolved SID experiments. Figure 3 compares TFECs obtained for these fragment ions. Interestingly, the kinetics of formation of all four common fragment ions from KYGGFL and RYGGFL are strikingly different with much faster kinetics observed for fragments of KYGGFL. In contrast, the appearance energies at long reaction delay times are quite similar for most fragments except for the b_2 ion, for which lower appearance energy is observed when RYGGFL is a precursor ion. The lower appearance energy of this fragment formed from RYGGFL suggests the threshold energy for the formation of

Table 2. Dissociation Parameters Obtained for Fragment Ions of KYGGFL, RYGGFL, and RYGGFL-OMe

	KYGGFL		RYGGFL		RYGGFL-OMe	
fragment	E_0, eV	$\Delta S^{\ddagger}$, eu[a]	E_0, eV	$\Delta S^{\ddagger}$, eu	E_0, eV	$\Delta S^{\ddagger}$, eu
$[M-NH_3+H]^+$			1.37	−16 (−9)	1.28	−19 (−11)
b_2	2.11	34 (23)[b]	1.26	−24 (−12)		
b_5	1.93	21 (13)	1.56	−11 (−6.5)		
$b_5 + H_2O$	2.48	55 (39)	1.95	22 (14)		
b_1	2.58	64 (47)	1.93	17 (11)	2.38	35 (23)

[a] eu = entropy units = cal/(mol K). [b] Activation entropy at 450 K; the value at 298 K is shown in parentheses for comparison with the literature. The estimated uncertainties are ±(5−10)% for the threshold energies and ±(3−8) eu for the activation entropies. Higher uncertainties are associated with reaction channels characterized by high activation entropy.

the b_2 ion from this precursor is lower than that for KYGGFL. Our results also suggest that b_1, b_2, b_5, and $b_5 + H_2O$ fragments of KYGGFL are formed via kinetically favorable pathways.

RRKM modeling of the data provides further support for this assertion. Table 2 compares modeling parameters obtained for the common primary fragments of KYGGFL, RYGGFL, and RYGGFL-OMe. Calculated TFECs are shown as solid lines in Figure 3, and calculated microcanonical rate constants are shown in Figure 4. The model provides a reasonable representation of the major trends in the experimental TFECs for all fragment ions. However, for several fragments, the agreement between the experimental data obtained at 1 ms reaction delay and model is not as good. It is reasonable to assume that at short reaction delay dissociation pathways characterized by higher threshold energies and kinetically favored fragmentation compete with slower channels that are dominant at long reaction delays. The deviation between the experiment and the model could be significantly reduced by introducing additional rate constants into the kinetic scheme. However, in this study, we attempted to use a minimum number of variable parameters in the model to eliminate redundancy. As a result, only dissociation parameters of lowest-energy pathways for each product ion are reported in this study.

For all common fragments of KYGGFL and RYGGFL, both the threshold energy and the activation entropy show a significant decrease when K is replaced with R in the sequence. These results indicate the formation of these fragments from KYGGFL follows kinetically favorable pathways with higher threshold energies, while fragmentation of RYGGFL follows lower-energy, kinetically hindered pathways. It is interesting to note that while similar dissociation parameters were obtained for the loss of NH_3 from the arginine side chain of RYGGFL and RYGGFL-OMe (Table 2), the energetics and dynamics of the b_1 ion formation from these two precursors are affected by methylation of the C-terminus.

HVYIHPF and RVYIHPF. Dissociation of RVYIHPF (Figure 5a) is dominated by the loss of NH_3 and the formation of b_n ($n = 1-6$), $b_n - NH_3$ ($n = 2-6$), a_n ($n = 2-5$), and $a_n - NH_3$ ($n = 2-5$) fragments,[47] while HVYIHPF yields an abundant b_5 ion corresponding to the enhanced cleavage at histidine[50,51] (His) and a number of b_n, $b_n - H_2O$ (b_n^o), and a_n ions (Figure 5c). In addition, the y_5 fragment is formed from both precursors. Note the much lower extent of fragmentation in the 75 eV SID

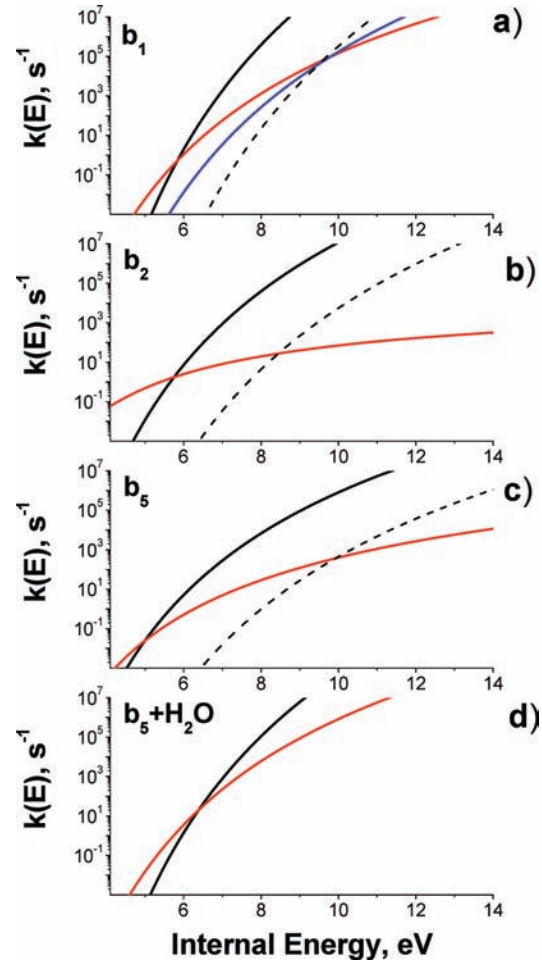

Figure 4. Microcanonical rate constants for the formation of b_1, b_2, b_5, and $b_5 + H_2O$ fragment ions of KYGGFL (black lines), RYGGFL (red lines), and RYGGFL-OMe (blue line). Dashed lines show rate constants of classical oxazolone pathways for the formation of these fragments from RYGGFL estimated by assuming threshold energies for dissociation of RYGGFL are ca. 0.5 eV higher than for KYGGFL, while activation entropies are the same as for KYGGFL (see text for more detail).

spectrum of RVYIHPF than observed in the 60 eV SID spectrum obtained using fluorinated SAM (FSAM) surface as SID target.[49b] The differences between the spectra are attributed to the differences in the vibrational-to-translation energy transfer efficiency upon collisions with FSAM (ca. 20%) and HSAM (ca. 10%) surfaces.[52] Detailed data analysis demonstrates that while RVYIHPF and HVYIHPF share a number of common fragment ions, only the b_5 and y_5 ions can be unambiguously attributed to products of primary fragmentation channels. Our previous study showed that $b_n - NH_3$ fragments of RVYIHPF result from sequential fragmentation of the primary $M-NH_3$ product ion.[49b] Appearance energy measurements for fragments of HVYIHPF suggest that smaller b_n ions are produced from the primary b_5 product ion.

C-terminal methylation has only a minor effect on the product ion distribution of RVYIHPF (Figure 5b and Figure S1 of the Supporting Information) and no effect on the types of fragments formed from HVYIHPF, indicating that dissociation pathways involving SB intermediates play no significant role for these precursor ions. The b_5 ion of RVYIHPF is not affected by the C-terminal methylation, while the y_5 ion is suppressed, indicating

(50) Farrugia, J. M.; O'Hair, R. A. J.; Reid, G. E. *Int. J. Mass Spectrom.* **2001**, *210*, 71–87.
(51) Tsaprailis, G.; Nair, H.; Zhong, W.; Kuppannan, K.; Futrell, J. H.; Wysocki, V. H. *Anal. Chem.* **2004**, *76*, 2083–2094.
(52) Laskin, J.; Futrell, J. H. *J. Chem. Phys.* **2003**, *119*, 3413–3420.

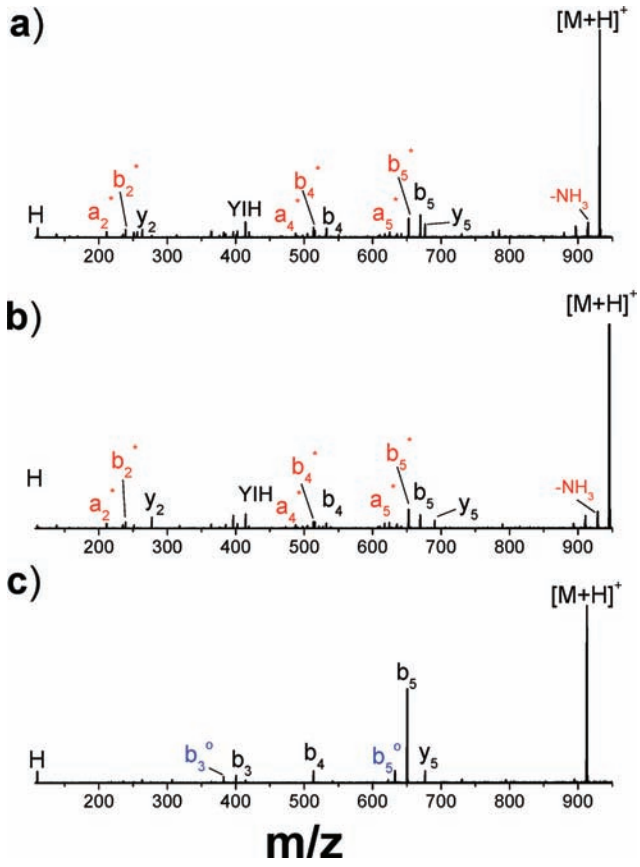

Figure 5. SID spectra corresponding to 50% fragmentation obtained on the HSAM surface at 1 s delay time for (a) RVYIHPF, 75 eV; (b) RVYIHPF-OMe, 75 eV; and (c) HVYIHPF, 51 eV ($b_n^* = b_n - NH_3$; $a_n^* = a_n - NH_3$; $b_n^o = b_n - H_2O$).

Table 3. Dissociation Parameters Obtained for Fragment Ions of HVYIHPF and RVYIHPF

	HVYIHPF		RVYIHPF	
fragment	E_0, eV	$\Delta S^{\ddagger}$, eu[a]	E_0, eV	$\Delta S^{\ddagger}$, eu
b_5	1.54	0.7 (0.3)	1.68	−11 (−6.5)
y_5	1.53	−7.4 (−3.9)	1.33	−28 (−14)

[a] eu = entropy units = cal/(mol K). Activation entropy at 450 K; the value at 298 K is shown in parentheses for comparison with the literature. The estimated uncertainties are ±(5−7)% for threshold energies and ±3 eu for activation entropies.

this pathway most likely proceeds through an SB intermediate. Alternatively, formation of the y_5 ion could be associated with the presence of histidine in the sequence. A recent study by Bythell et al.[53] demonstrated that for polyalanine peptides containing one histidine residue y-ions are formed when histidine is positioned at least two amino acids away from the N-terminus. Threshold energies and activation entropies obtained for these fragments are summarized in Table 3. Experimental TFECs and the corresponding modeling results are shown in Figure 6.

Dramatically different kinetic behavior is observed for the formation of these fragment ions from the two precursors, indicating significant differences in entropy effects. Similar to results obtained for YGGFL derivatives, the formation of the b_5 and y_5 backbone fragments from RVYIHPF is kinetically

(53) Bythell, B. J.; Knapp-Mohammady, M.; Paizs, B.; Harrison, A. G. *J. Am. Soc. Mass Spectrom.* **2010**, *8*, 1352−1363.

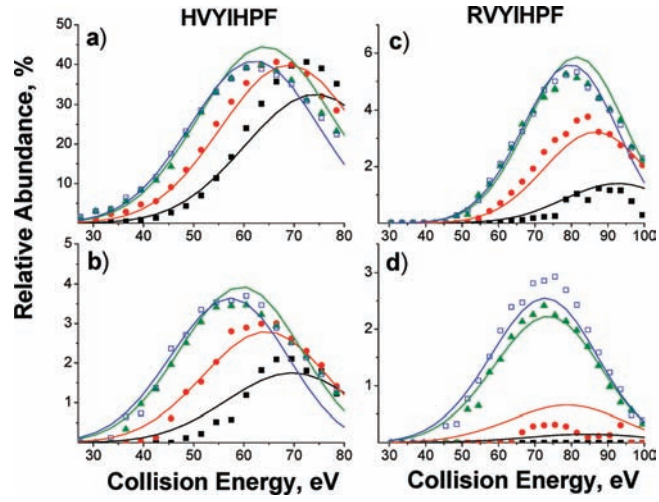

Figure 6. TFECs obtained for the b_5 (a,c) and y_5 fragments (b,d) of HVYIHPF (left) and RVYIHPF (right), respectively. The results are shown for delay times of 1 ms (■), 10 ms (red ●), 100 ms (green ▲), and 1 s (blue □). Solid lines show RRKM modeling results for the corresponding delay times.

hindered. The RRKM modeling shows a 0.15 eV increase in the threshold energy for the b_5 ion formation and a 0.2 eV decrease in the threshold energy for the y_5 ion formation from RVYIHPF as compared to HVYIHPF, while activation entropies are consistently more negative in the presence of arginine.

Theoretical Results. Low-energy structures of singly protonated KYGGFL and RYGGFL are shown in Figure 7. For both KYGGFL and RYGGFL, the ionizing proton resides on the side chains of basic residues and is solvated by a number of backbone carbonyl groups. Figure 7 shows the protonated lysine side chain is stabilized by four strong hydrogen bonds, and the protonated guanidino group is stabilized by five weaker bonds.

Figure 8 shows lowest-energy structures of protonated RVYIHPF and HVYIHPF. The protonated arginine side chain of RVYIHPF (Figure 8a) is stabilized by six hydrogen-bonding interactions with the third, fifth, and sixth backbone carbonyl groups. In the absence of the basic arginine residue in HVYIHPF, the ionizing proton can reside either on the first or on the fifth histidine residue. DFT calculations indicate that low-energy structures of HVYIHPF ionized on His^1 and His^5 have comparable stabilities, suggesting that both structures shown in Figure 8b and c, respectively, may coexist in the gas phase. It is interesting to note that while the protonated arginine side chain of $[RVYIHPF+H]^+$ is heavily solvated by backbone carbonyl groups, the protonated histidine side chains of both $[His^1VYIHPF+H]^+$ and $[HVYIHis^5PF+H]^+$ form fewer hydrogen bonds. The protonated His^1 is solvated by the first, third, and sixth backbone carbonyl groups, while the protonated His^5 interacts with the fifth and sixth backbone carbonyls.

Discussion

Dissociation Pathways. The results presented in this study demonstrate that replacing arginine with a less basic residue in a peptide sequence has a dramatic effect on the observed fragmentation behavior. Few common primary fragments were observed for the two pairs of model systems studied here (RYGGFL and KYGGFL, RVYIHPF and HVYIHPF). However, each arginine-containing species showed distinctly different fragmentation behavior. For example, pathways involving SB intermediates play an important role in dissociation of RYGGFL.

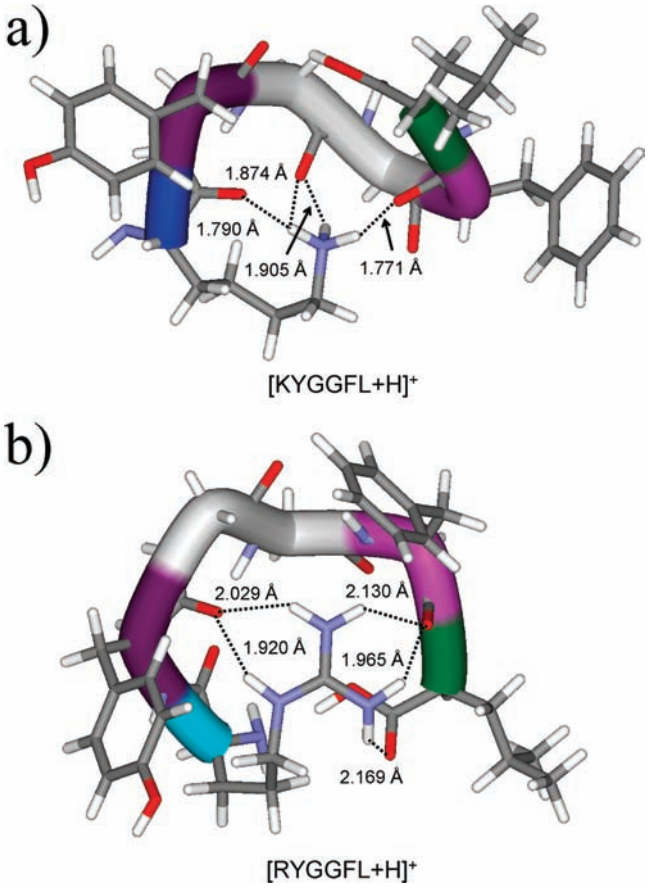

Figure 7. Lowest-energy structures of (a) $[KYGGFL+H]^+$ and (b) $[RYGGFL+H]^+$. Peptide backbone is shown as colored tubes. Dotted lines indicate hydrogen bonds solvating the protonation site.

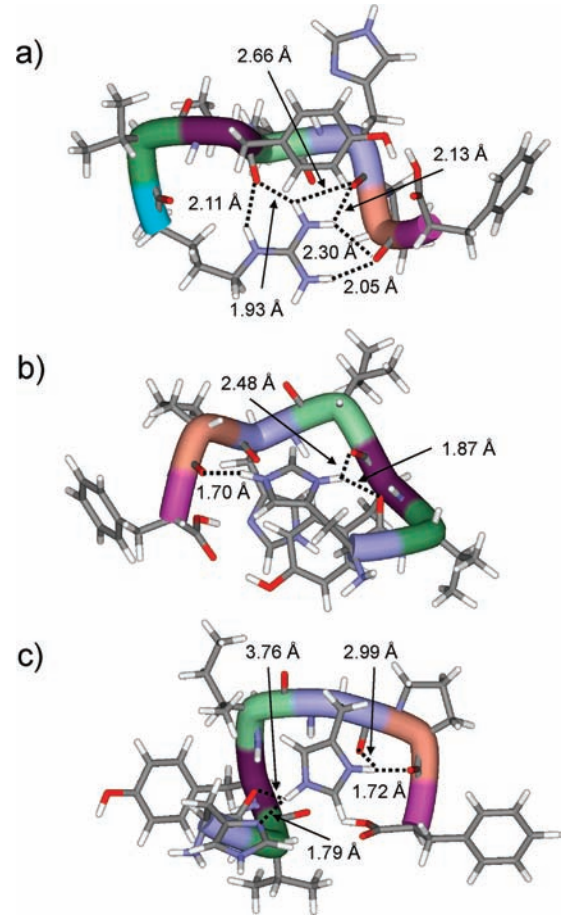

Figure 8. Lowest-energy structures of (a) $[RVYIHPF+H]^+$, (b) $[HVYIHPF+H]^+$ protonated at His^1, and (c) $[HVYIHPF+H]^+$ protonated at His^5. Peptide backbone is shown as colored tubes. Dotted lines indicate hydrogen bonds solvating the protonation site.

This was confirmed by blocking the C-terminal carboxyl group, which resulted in suppression of a significant number of backbone fragments. In contrast, methylation of the C-terminus of RVYIHPF suppressed only two minor fragments, y_5 and $b_6 + H_2O$, indicating the proton of the C-terminal carboxyl group of this peptide is not involved in dissociation. A similar approach was used to confirm that dissociation of KYGGFL and HVYIHPF follows pathways involving canonical structures. In the absence of pathways involving SB intermediates, fragmentation of arginine-containing peptides (RYGGFL-OMe and RVYIHPF) is dominated by the loss of NH_3. This reaction channel was not observed for KYGGFL and HVYIHPF.

The presence of the basic arginine in the sequence also has a significant effect on the kinetics of dissociation (Figures 3 and 6) with much faster kinetics observed when arginine is replaced with a less basic residue. As a result, the activation entropy of the total decomposition is higher for peptides lacking the arginine residue, whereas threshold energies do not show a clear pattern (Table 1). From the previous discussion, it follows that observed differences in the relative stabilities of the four peptides largely reflect differences in the dissociation pathways. This conclusion is consistent with previous work by Vachet and Glish[22] who proposed that differences between gas-phase fragmentation of peptides with and without arginine may be attributed to the predominance of different reaction mechanisms (e.g., charge-directed in the absence of arginine and charge-remote in the presence of arginine). However, for the series of peptides examined in this study, we demonstrate that the competition between different charge-driven rather than charge-remote pathways determines the relative stability of arginine-containing peptides as compared to their analogues containing less basic histidine and lysine residues. RRKM modeling results (discussed as follows) provide a framework for detailed understanding of the competition between different dissociation channels.

Dissociation Parameters of SB Pathways. Comparison between dissociation parameters obtained for common reaction products of the two pairs of peptides examined in this study (Tables 2 and 3) demonstrates that fragmentation of arginine-containing peptides is associated with lower dissociation barriers and fairly tight transition states. For example, strikingly different dissociation parameters were obtained for the formation of the b_2 and b_5 ions from RYGGFL and KYGGFL with much higher threshold energies and large positive activation entropies obtained for KYGGFL. Specifically, the threshold energy increased from 1.26 to 2.11 eV for the b_2 ion and from 1.56 to 1.93 eV for the b_5 ion. The activation entropies increased from -24 to 34 eu for the b_2 ion and from -11 to 21 eu for the b_5 ion. Similar trends in dissociation parameters were obtained for the y_5 fragment ion of RVYIHPF (1.33 eV, -28 eu) and HVYIHPF (1.53 eV, -7.4 eu). As discussed earlier, these fragment ions are produced through pathways involving SB intermediates when arginine is present in the sequence and through classical pathways in the absence of arginine. Thus, it follows that pathways involving SB intermediates are associated

with lower dissociation barriers and more negative activation entropies. This conclusion is in qualitative agreement with the computational study by Paizs and co-workers[35] that examined dissociation of singly protonated G_nR ($n = 1-4$) peptides. Interestingly, 298 K activation entropies obtained in this study (Table 2) are quite similar to the values reported by Paizs and co-workers. For example, the calculated activation entropies for cleavages of amide bonds of $[GGGGR+H]^+$ are in the range of −18.6 to −13.5 eu at 298 K both for anhydride and for SB pathways, whereas the experimental values at 298 K determined in this study are in the range of −14 to −6.5 eu.

The b_5 Fragment Ion of RVYIHPF and HVYIHPF. Wysocki and co-workers proposed that backbone fragmentation of the singly protonated RVYIHPF is not directed by the histidine side chain.[51] Because the b_5 ion formation from RVYIHPF was not affected by methylation of the C-terminal carboxyl group, it is reasonable to assume this fragment ion is formed through a canonical pathway. However, the dissociation parameters obtained for this product ion (Table 3) are still strongly affected by the presence of arginine. In the following, we will discuss the most plausible explanation of the observed differences of the kinetics of formation of the b_5 ion. It is interesting to note that while the b_5 ion of HVYIHPF is the most abundant primary product ion with the maximum relative abundance of ca. 40%, the relative abundance of the b_5 ion formed from RVYIHPF does not exceed 6%. The enhanced formation of the b_5 ion from HVYIHPF is consistent with the mechanism proposed in the literature.[50,51] It has been demonstrated that the enhanced cleavage at histidine occurs when the ionizing proton resides on the imidazole ring of the histidine side chain.[50,51] The mechanism involves transfer of the ionizing proton to the C-terminal amide oxygen followed by nucleophilic attack by the imino nitrogen on the carbonyl carbon. As discussed earlier, the structure of HVYIHPF protonated at His^5 coexists with the structure protonated at His^1 in the gas phase. The b_5 ion is most likely formed from HVYIHPF structures protonated at His^5 via the mechanism that involves the imidazole side chain. In contrast, the formation of the b_5 fragment from RVYIHPF protonated at the guanidino group of R most likely follows the canonical pathway.[5]

On the basis of the previous discussion, it follows that the b_5 fragment of RVYIHPF and HVYIHPF is produced through different mechanisms. Modeling results shown in Table 3 indicate the formation of the b_5 ion through a canonical pathway is characterized by the more negative activation entropy. It follows that this pathway is associated with more significant rearrangement than the mechanism involving the protonated histidine side chain.

The Energetics and Dynamics of Formation of $b_n + H_2O$ Ions. Loss of the C-terminal amino acid residue resulting in formation of $b_n + H_2O$ ions is typical for protonated peptides with arginine at the C-terminus. This pathway requires the presence of a carboxyl group at the C-terminus and proceeds through an SB intermediate. Gaskell and co-workers used CID and ^{18}O labeling experiments to demonstrate that the resulting $b_n + H_2O$ fragments retain one of the carboxyl oxygens and are indistinguishable from the corresponding peptides with one fewer amino acid residues.[28,29] Gonzalez et al.[30] showed that the position of the basic amino acid residue and its basicity have a significant effect on the C-terminal rearrangement. They demonstrated that the relative abundance of $b_n + H_2O$ fragments decreases when arginine is replaced with a less basic lysine residue and that the rearrangement product is particularly abundant when arginine is in the $(n - 1)$ position.

While the formation of the $b_n + H_2O$ ion has been extensively studied both for protonated peptides[28−30] and for peptide cationized on metals,[54−56] the energetics of this pathway has not been explored. In this study, we present for the first time the energetics and dynamics of formation of $b_n + H_2O$ fragment ions. Dissociation thresholds for the formation of the $b_5 + H_2O$ of 2.48 and 1.95 eV were obtained for KYGGFL and RYGGFL, respectively, with corresponding 450 K activation entropies of 55 and 22 eu, respectively. Because the formation of the $b_5 + H_2O$ ion requires substantial rearrangement,[28−30] high positive activation entropies obtained for this reaction channel are quite surprising. This observation can be rationalized by assuming that while the formation of this fragment ion involves the initial rearrangement step, the rate-determining step of the process is characterized by high threshold energy and a fairly loose transition state.

The Formation of b_1 Ions. In this study, abundant b_1 ions were observed as primary products of the gas-phase fragmentation of protonated RYGGFL and KYGGFL. This observation is consistent with previous work from several groups that examined structures and stabilities of b_1 fragments of amino acids and peptides. It has been demonstrated that while acylium b_1 ions of amino acids are inherently unstable with respect to CO loss,[57−59] stable cyclic b_1 ions are formed via neighboring group interaction pathways involving side chains of arginine,[60] lysine,[61] histidine,[62] and methionine.[63] Because the formation of stable cyclic b_1 ions requires substantial rearrangement, the corresponding cleavage of the amide bond must be characterized by a tight transition state. However, similar to the formation of $b_n + H_2O$ fragments discussed earlier, the formation of b_1 products of RYGGFL and KYGGFL is characterized by loose transition states and high energy barriers. These results indicate cleavage of the amide bond is not the rate-determining step for this dissociation channel. It is interesting to note that the C-terminal methylation of RYGGFL increases the dissociation threshold for the formation of the b_1 ion, indicating that this product may be formed through two different reaction pathways when RYGGFL is a precursor ion, a pathway involving arginine side chain and a pathway involving the C-terminal proton.

The Competition between the SB and Canonical Pathways. The results presented in this study clearly demonstrate that kinetically hindered fragmentation channels of arginine-containing peptides involving SB intermediates efficiently compete with classical pathways on a long time scale of an FTICR-MS. However, fragmentation channels characterized by high activation entropies may become favorable when MS/MS experiments

(54) Grese, R. P.; Cerny, R. L.; Gross, M. L. *J. Am. Chem. Soc.* **1989**, *111*, 2835–2842.
(55) Teesch, L. M.; Adams, J. *J. Am. Chem. Soc.* **1990**, *112*, 4110–4120.
(56) Lee, S. W.; Kim, H. S.; Beauchamp, J. L. *J. Am. Chem. Soc.* **1998**, *120*, 3188–3195.
(57) Harrison, A. G. *Mass Spectrom. Rev.* **2009**, *28*, 640–654.
(58) Tsang, C. W.; Harrison, A. G. *J. Am. Chem. Soc.* **1976**, *98*, 1301–1308.
(59) O'Hair, R. A. J.; Reid, G. E. *Rapid Commun. Mass Spectrom.* **2000**, *14*, 1220–1225.
(60) Hiserodt, R. D.; Brown, S. M.; Swijter, D. F. H.; Hawkins, N.; Mussinan, C. J. *J. Am. Soc. Mass. Spectrom.* **2007**, *18*, 1414–1422.
(61) Yalcin, T.; Harrison, A. G. *J. Mass Spectrom.* **1996**, *31*, 1237–1243.
(62) Farrugia, J. M.; Taverner, T.; O'Hair, R. A. J. *Int. J. Mass Spectrom.* **2001**, *209*, 99–112.
(63) Tu, Y. P.; Harrison, A. G. *Rapid Commun. Mass Spectrom.* **1998**, *12*, 849–851.

are performed on a shorter time scale. For example, Forbes et al. compared CID spectra of GR and RG obtained using different mass analyzers.[64] They showed that rearrangement to the anhydride intermediate, a dominant pathway in ion trap experiments of Farrugia and O'Hair,[31] does not occur in the quadrupole/quadrupole/time-of-flight (QqTOF) instrument. This behavior was attributed to the shorter observation time and higher excitation energy in the QqTOF MS/MS experiments as compared to the ion trap.

Figure 4 compares microcanonical rate constants obtained for common fragments of RYGGFL, RYGGFL-OMe, and KYGGFL. Because of lower dissociation thresholds and more negative activation entropies characteristic of all dissociation channels of RYGGFL, microcanonical rate constants for dissociation of this precursor originate at lower internal energies and increase much more slowly than the rate constants obtained for KYGGFL. The crossing points between rate-energy curves of RYGGFL and KYGGFL occur at $0.02-30\ s^{-1}$, indicating that dissociation of KYGGFL is generally faster even on the long time scale of an FTICR instrument. Kinetically hindered fragmentation of RYGGFL is mainly attributed to the dominance of SB pathways generally associated with substantial rearrangement.[35]

Rate-energy dependencies of canonical pathways of RYGGFL were estimated from microcanonical rate constants obtained for KYGGFL, assuming the threshold energy for dissociation of RYGGFL is higher than that for KYGGFL by the difference in proton affinities of arginine and lysine. The resulting rate constants obtained using positive activation entropies of dissociation channels of KYGGFL and 0.5 eV higher threshold energies are shown as dashed lines in Figure 4. Interestingly, the rate-energy dependency obtained for the b_1 ion formation from RYGGFL-OMe via the canonical pathway is in a good qualitative agreement with the estimated rate-energy curve for RYGGFL (Figure 4a), indicating the validity of this approach. Also, in agreement with the study by Forbes et al.,[64] our results show that fast fragmentation becomes dominant at high internal excitation and short reaction times. The estimated crossing point is 9.5 eV and $5 \times 10^4\ s^{-1}$ for the b_1 ion, 8.5 eV and $30\ s^{-1}$ for the b_2 ion, and 9.9 eV and $300\ s^{-1}$ for the b_5 ion, indicating that the competition between the SB and canonical pathways depends on the type of the fragment ion. On the basis of the T→V conversion efficiency of 8.8% for collisions with the HSAM surface obtained from the RRKM modeling, we estimate that the canonical pathways should become dominant in our SID experiments at collision energies above ca. 95 eV. Because canonical dissociation pathways of RYGGFL are important only at very high collision energies, incorporation of the estimated microcanonical rate constants into the RRKM modeling of SID data had no significant effect on the quality of the fit.

In contrast, SB pathways play only a minor role in gas-phase fragmentation of the protonated RVYIHPF. As discussed in our previous study, the stability of this peptide toward fragmentation is largely determined by the loss of ammonia from the arginine side chain.[49b] While it is difficult to explain the observed differences in fragmentation behavior of RYGGFL and RVYIHPF, we hypothesize that the secondary structure of the peptide may play an important role in determining the extent of competition between dissociation pathways involving SB intermediates and canonical structures. Indeed, we note that the C-terminus of RYGGFL is solvated by the protonated arginine side chain as shown in Figure 7b. This interaction is important for efficient solvation of the deprotonated carboxyl group in the transition state involved in the proton-transfer process.[35] In contrast, the protonated guanidino group of RVYIHPF is solvated by the backbone carbonyls rather than by the C-terminal carboxyl group (Figure 8a). It is reasonable to assume that the proton transfer from the carboxyl group of RVYIHPF is kinetically more hindered than the formation of the SB structure of RYGGFL, which could account for the reduced role of SB pathways in dissociation of RVYIHPF.

Conclusions

We have performed a detailed investigation of the effect of the basic amino acid residue on the energetics, dynamics, and mechanisms of dissociation of protonated peptides in the gas phase using time- and collision energy-resolved SID experiments. Substitution of histidine or lysine with more basic arginine residue has a dramatic effect on the types and mechanisms of formation of peptide fragments. Specifically, we found that there is little overlap between SID spectra of peptides with and without arginine residue and that common fragments are often produced through different mechanisms. For example, b_1, b_2, and b_5 fragments of RYGGFL are formed via mechanisms that involve SB intermediates, while the formation of these fragments from KYGGFL proceeds through channels involving canonical structures. Similarly, the mechanisms of formation of b_5 and y_5 fragments of RVYIHPF and HVYIHPF are quite different. Methylation of the C-terminal carboxyl group allowed us to distinguish between different pathways and obtain dissociation parameters using RRKM modeling of the experimental data. Substitution of the tyrosine residue with phenylalanine helped rule out possible involvement of SB structures that originate from the abstraction of the acidic phenolic proton.

Time-resolved and collision energy-resolved SID data showed that pathways involving SB intermediates are kinetically hindered as compared to canonical pathways. This finding was confirmed using detailed RRKM modeling of the experimental SID data that provided the first experimental determination of energy and entropy effects associated with SB pathways. The surprising finding reported in this study is that dissociation of arginine-containing peptides is often characterized by lower threshold energies than fragmentation of their histidine- and lysine-containing analogues. However, because of the lower activation entropies obtained for these precursor ions, their fragmentation is slow. As a result, higher internal excitations are required to observe dissociation of arginine-containing peptides in a mass spectrometer. This study provides additional support for the important role of the activation entropy in the gas-phase fragmentation of peptide ions. On the basis of our previous work,[8,20] we anticipate that collision-induced dissociation (CID) commonly used in practical applications will sample similar dissociation pathways as long as the experimental time scale is comparable to our SID experiments. We also demonstrated that, in agreement with the mobile proton model, classical oxazolone fragmentation pathways of arginine-containing peptides are associated with higher threshold energies and similar entropy effects as compared to their lysine- and histidine-containing analogues. Qualitative agreement between dissociation parameters obtained in this study and parameters reported in the computational study by Paizs and co-workers[35] for small $[G_nR+H]^+$ indicate that the competition between SB and

(64) Forbes, M. W.; Jockusch, R. A.; Young, A. B.; Harrison, A. G. *J. Am. Soc. Mass Spectrom.* **2007**, *18*, 1959–1966.

canonical pathways discussed in this study is a rather general phenomenon relevant to peptide sequencing.

Acknowledgment. This study was partially supported by the grant from the Division of Chemical Sciences, Geosciences, and Biosciences, Office of Basic Energy Sciences of the U.S. Department of Energy (DOE), and the University of Hong Kong and Hong Kong Research Grant Council, Special Administrative Region, China (Project No. 7012/08P). The research described in this article was performed at the DOE's W.R. Wiley Environmental Molecular Sciences Laboratory (EMSL), a national scientific user facility sponsored by the DOE's Office of Biological and Environmental Research and located at Pacific Northwest National Laboratory (PNNL). PNNL is operated by Battelle for the DOE under Contract DE-AC05-76RL01830.

Supporting Information Available: Complete ref 43. 90 eV SID spectra of RVYIHPF and RVYIHPF-OMe. This material is available free of charge via the Internet at http://pubs.acs.org.

JA104438Z